ELSEVIER

Journal of Structural Geology 27 (2005) 645–661

JOURNAL OF STRUCTURAL GEOLOGY

www.elsevier.com/locate/jsg

The control of precursor brittle fracture and fluid–rock interaction on the development of single and paired ductile shear zones

Neil S. Mancktelow[a,*], Giorgio Pennacchioni[b,c]

[a]*Geologisches Institut, ETH-Zentrum, CH-8092 Zürich, Switzerland*
[b]*Dipartimento di Geologia, Paleontologia e Geofisica, Univ. di Padova, I-35137 Padova, Italy*
[c]*CNR Instituto di Geoscienze e Georisorse (Sezione di Padova), Padova, Italy*

Received 2 July 2004; received in revised form 10 November 2004; accepted 17 November 2004
Available online 19 January 2005

Abstract

Ductile shear zones can occur as relatively isolated single structures, as arrays, or as characteristic paired zones. In continuous glaciated exposures of metagranodiorites from the Tauern window (Eastern Alps), the control of initial dilatant brittle fracture and associated fluid–rock interaction on the geometry of subsequent ductile shear zones can be unequivocally established. Shearing occurred under amphibolite facies conditions. Fractures in weakly deformed metagranodiorites are often less than 1 mm thick but extend for tens of metres. Many are healed joints without shear offset. Others show minor (mm–cm), discrete dextral offset. Such brittle faults commonly display a low-angle en-échelon arrangement, with displacement transferred between discrete fracture segments by ductile compressive bridges. The geometry of more strongly reactivated zones depends on the degree and heterogeneity of fluid–rock interaction, which is related to fluid infiltration and veining along the primary fractures. With little fluid–rock interaction, reactivation produces single heterogeneous ductile shear zones centred on and immediately flanking the pre-existing fracture. With increased fluid–rock interaction, a bleached halo is developed symmetrically to either side of a central epidote–quartz ($\pm$garnet $\pm$calcite) vein. Ductile shear zones commonly flank this bleached zone, to develop a characteristic paired pattern. Strain is partitioned, localizing in the central fracture/vein and the flanking shear zones. Paired zones may anastomose in accordance with changes in the width of the central bleached zone, but are always symmetrically spaced with regard to the central fracture/vein. With increasing deformation, the ductile shear zones broaden into the adjacent metagranodiorite but not into the bleached zone, which remains preserved as a low strain region. Paired shear zones can also develop to either side of aplite dykes. Examples of characteristic paired shear zones, usually with a clear central vein, are found in many areas ranging from greenschist to eclogite facies, suggesting that the mechanism of their formation is quite general.

Keywords: Shear zones; Fluid–rock interaction; Brittle–ductile deformation; Fracture reactivation; Tauern window; European Alps

1. Introduction

Heterogeneous ductile shear zones occur in deformed rocks on all scales and are recognizable from their characteristic sigmoidal foliation pattern (e.g. figs. 3.3 and 3.4 of Ramsay and Huber, 1983). They are particularly clearly developed, and their geometry, kinematics and associated chemical/mineralogical changes most easily studied, in homogeneous plutonic bodies (Ramsay and Graham, 1970; Burg and Laurent, 1978; Simpson, 1983; Vauchez, 1987; Selverstone et al., 1991; Dutruge et al., 1995; Christiansen and Pollard, 1997; Arbaret and Burg, 2003; Rolland et al., 2003). However, heterogeneous shear zones have been described from a wide range of crustal rocks (Carreras and Garcia Celma, 1982; Pennacchioni, 1996; Bestmann et al., 2000) and are also important in mantle deformation (Müntener and Hermann, 1996; Van der Wal and Vissers, 1996).

Shear zones are long relative to their width and in many studies have been approximated as banded structures that are effectively invariant along their length (e.g. Ramsay and Graham, 1970; Cobbold, 1977a,b; Casey, 1980). As discussed by Ramsay and Graham (1970), the

* Corresponding author. Tel.: +41-44-632-3671; fax: +41-44-632-1030
E-mail address: neil@erdw.ethz.ch (N.S. Mancktelow).

0191-8141/$ - see front matter © 2005 Elsevier Ltd. All rights reserved.
doi:10.1016/j.jsg.2004.12.001

heterogeneous strain component in such a banded structure can only be due to variation in band-parallel simple shear or band-perpendicular contraction or extension due to volume change. Stress equilibrium requires that the shear stress parallel to the band and the normal stress perpendicular to the band are constant throughout (Cobbold, 1977b). If the original protolith is homogeneous, the heterogeneous strain component must therefore reflect a change in material properties related to deformation.

It is commonly argued that progressive deformation leads to strain softening, due to dynamic recrystallization and associated grain size reduction, development of crystallographic preferred orientation, or synkinematic mineral transformations, e.g. of feldspar to muscovite and 'phyllonitization' (Bowden, 1970; Poirier, 1980; White et al., 1980; Williams and Dixon, 1982; Gilotti and Kumpulainen, 1986; Hobbs et al., 1990). Weakening and localization is then a direct result of increasing deformation. The characteristic sigmoidal foliation pattern reflects an increasing localization of shear strain toward the median line of the shear zone. It follows that deformation should become spatially more heterogeneous with time.

A radically different explanation for localized shear zones in deformed granitoids has been more recently proposed (Simpson, 1985, 1986; Segall and Simpson, 1986; Tremblay and Malo, 1991; Tourigny and Tremblay, 1997; Guermani and Pennacchioni, 1998, Pennacchioni, 2005). In this model, extreme localization related to brittle fracture is the necessary precursor to shear zone development. The brittle fractures control the location and therefore the geometry of the subsequent ductile shear zones. Shear zones develop by broadening, reflecting a transition to more distributed ductile deformation. The transition to ductile behaviour is promoted by mineral transformation resulting from fluid influx along the precursor fracture. In this model, the shear zones are most localized in the initial precursor brittle stage and broaden during subsequent ductile reactivation.

Natural ductile shear zones have been described either as relatively isolated structures or forming subparallel to anastomosing arrays (e.g. Ramsay and Allison, 1979; Arbaret and Burg, 2003). However, what has not previously been specifically described is the characteristic development of paired zones, in which a near parallel set of two shear zones develops. The spacing between the individual shear zones is small relative both to the length of the shear zone pair and to the distance to the next adjacent paired or single zone (Fig. 1). Here we describe in detail the geometry of particularly well-exposed examples developed in metagranodiorites from the Tauern window of the eastern European Alps. However, such paired shear zones have been observed in a wide range of rocks and deformation environments (Fig. 2; see also fig. 4 of Segall and Simpson, 1986). This characteristic paired geometry is so common that it must reflect a general process of shear zone nucleation.

Fig. 1. Paired shear zone from the Am Mösele area, South Tyrol (looking east, 46° 58′ 23.9″, 11° 47′ 45.7″).

This paper establishes that both single and paired shear zones can develop from precursor brittle fractures and that the geometry of the shear zones reflects the initial fracture geometry and the influence of fluid infiltration along the fracture. The area described, with its almost continuous polished exposures, allows the transition from an initial brittle precursor to a 'mature' ductile shear zone to be carefully documented, as well as the relationship between fracture, fluid–rock interaction, and shear zone localization. The type of fluid–rock interaction occurring along the brittle precursor structures controls the geometry of the developing shear zones, and ultimately determines whether single or paired zones are developed.

2. Regional geology and rock types

The outcrop investigated in this study is a polished glaciated surface immediately below the 'Östlicher Nöfesferner' glacier east of 'Am Mösele' in South Tyrol, Italy (46° 58′ 23.2″, 11° 47′ 48.6″, GPS relative to WGS84). It forms part of the Zillertal–Venediger Massif, one of the

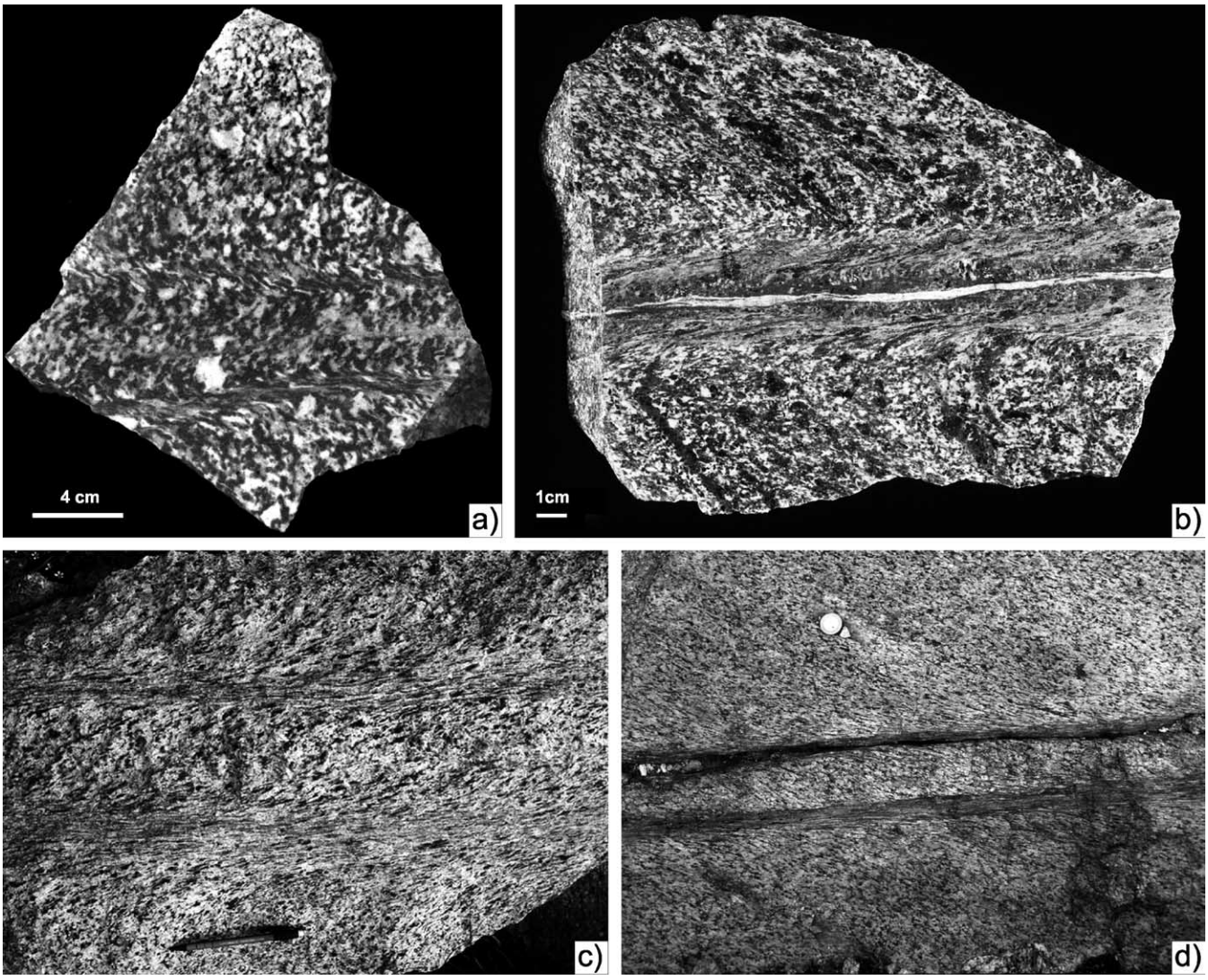

Fig. 2. (a) Paired shear zone developed symmetrically to either side of a central Mn-epidote-rich vein, Mucrone area, western Alps. (b) Eclogite facies paired shear zones with central epidote-rich vein, developed in mafic granulites of the Mt Emilius Austroalpine unit, western Alps (Pennacchioni, 1996). (c) Paired shear zones in orthogneiss, Laghetti, Central Alps (Swiss Coords 147200/688538). (d) Sinistral paired shear zone from the Am Mösele area (this study), without a discernible central vein (46° 58′ 15.6″, 11° 47′ 45.7″). Shear zones further north, as considered here, are predominantly dextral.

three main cores of the Central Gneisses (or 'Zentralgneise') within the Penninic Lower Schieferhülle unit of the Tauern window in the Eastern Alps. This unit largely consists of a series of late- to post-Hercynian (ca. 310–290 Ma) intrusions, volumetrically dominated by calc–alkaline I-type tonalites, granodiorites and granites (e.g. Finger et al., 1993, 1997). In the studied area, the main body is a medium-grained (mm grain size), rather equigranular biotite-bearing granodiorite (quartz–plagioclase–biotite ± K-feldspar ± muscovite) with enclaves of more basic composition. The intrusion generally preserves a NS-trending and steeply dipping magmatic fabric, defined by a shape preferred orientation of planar trains of biotite and feldspar phenocrysts and by the marked elongation of basic enclaves. This major composite pluton was intruded, from oldest to youngest, by finer-grained leucocratic granitoids, porphyritic amphibole–biotite-bearing lamprophyres and aplitic dykes.

The Tauern window has a polyphase pre-Alpine and Alpine history of metamorphism and deformation (Lammerer, 1988; von Blanckenburg et al., 1989; Lammerer and Weger, 1998). The pre-Alpine history includes an early- to pre-Hercynian high-pressure event recorded by zoisite segregation (Brunsmann et al., 2000) followed by Hercynian conditions of ca. 0.7 GPa/600 °C. The Alpine evolution consists of an early blueschist to eclogite-facies event (0.9–1.2 GPa/450 ± 50 °C) (Selverstone, 1984) followed by decompression, with a thermal peak attained during the Oligocene 'Tauern metamorphism' (0.5–0.7 GPa/500–650 °C) (Hoernes and Friedrichsen, 1974; Friedrichsen and Morteani, 1979). This latter phase produced pervasive static recrystallization within the Lower Schieferhülle

(Morteani, 1974). Final cooling only occurred during Oligocene to Neogene exhumation of the Tauern window (Selverstone and Spear, 1985; Selverstone, 1988; Fügenschuh et al., 1997). In the studied area, maximum temperatures during the Tauern metamorphism were on the order of 550–600 °C (Hoernes and Friedrichsen, 1974).

The major part of the studied plutonic body shows little macroscopic evidence of deformation and metamorphism and igneous relationships are well preserved. Here we specifically consider the isolated and rather discrete initial deformation structures that develop. Locally, the transition to more widespread foliation development can also be observed. This is especially true toward the south, where there is a rapid but gradational transition to a km-scale sinistral strike-slip mylonitic zone that forms the southern margin of the Zillertal–Venediger Massif. This broad shear zone continues across the contact to the overlying Austroalpine nappes (e.g. see map of De Vecchi and Mezzacasa, 1986), demonstrating that it is of Alpine age. The dominant, generally E–W-striking shear zones in the region show both dextral (see below) and sinistral (Fig. 2d) shear senses, with dextral senses more common toward the north. In the studied area, mutually cross-cutting relationships indicate broad contemporaneity, but regionally there is a demonstrable transition from sinistral to dextral shear with initiation of the regional Periadriatic Fault system in the mid-Oligocene, around 32 Ma (Mancktelow et al., 2001; Müller et al., 2001).

3. Mesoscale features of incipient brittle-to-ductile deformation

3.1. Precursor fractures and incipient ductile reactivation

In the least deformed areas, metagranodiorites without any mesoscopic evidence of solid state deformation are crosscut by isolated, knife-sharp (<1–2 mm wide) fractures (Fig. 3), which may have a strike length of many tens of metres (Fig. 4a). In more deformed areas, the fractures form closely spaced networks arranged in different sets, which usually display incipient to relatively strong ductile reactivation. Three main nearly vertical fracture sets are observed: one striking ca. EW, one ca. NS and one ca. NE–SW. The EW set is the most common and that which most frequently shows a transition to ductile shearing. The other two sets (NS and NE–SW) are not generally strongly reactivated. The NS set shows minor sinistral offset, when observed, and is typically marked by relatively thick quartz–calcite–plagioclase–biotite veins (e.g. Cesare et al., 2001), which terminate in dilational wing cracks (cf. fig. 8a of Segall and Pollard, 1983). In the following, we consider only the relationship between brittle and ductile shearing on the best-developed EW set.

Most fractures show no discernible offset of crosscutting markers (e.g. aplitic dykes, basic enclaves or biotite-rich layers; Fig. 3a). However, in some cases, along the same fracture the marker offset varies from zero (Fig. 3a) to a few centimetres (Fig. 3b) even though no foliation is developed in the immediately adjacent granodiorite. The fractures are usually marked by a dark biotite-rich seam. This seam is more evident where there is some offset. Along some short segments, the fractures may be perfectly healed without any discernible seam and the macroscopic trace may be difficult to identify. However, irregularly distributed iron staining is common along fractures and highlights their trace on polished outcrops (Fig. 4a). Some fractures show an irregular enrichment in biotite in the adjacent host granite to form a narrow halo on the mm–cm scale.

Along fractures there is commonly a progressive transition from (1) joints without discernible shear offset (Fig. 3a), to (2) knife-sharp faults displaying minor offset within apparently undeformed granite (Fig. 3b), to (3) shear fractures associated with a weak, nearly straight foliation inclined at ca. 45° to the fracture and extending for millimetres to a few centimetres into the adjacent country rock (Fig. 4b and c), to (4) bands, several centimetres wide, of sigmoidally shaped foliation typical of heterogeneous

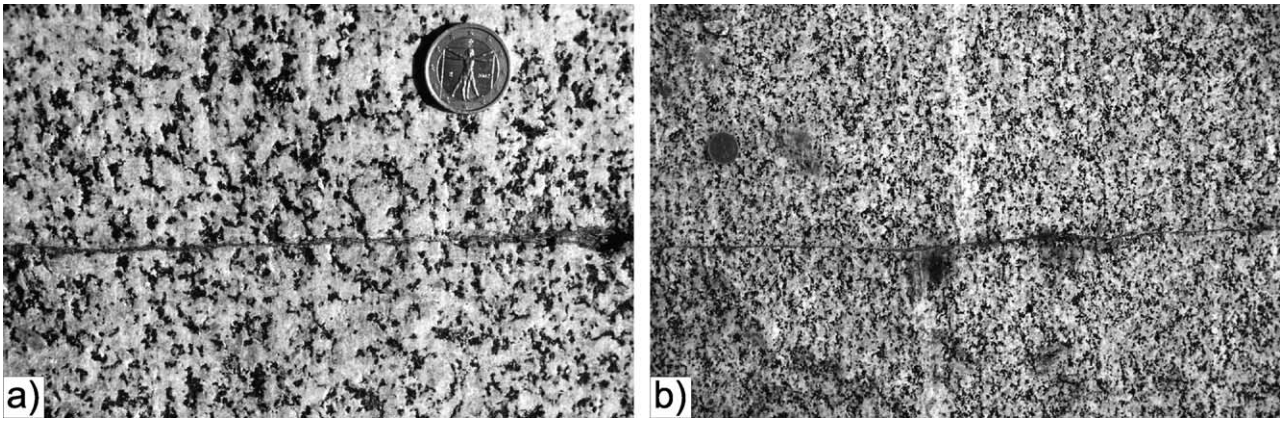

Fig. 3. Incipient reactivation of discrete fractures (the fractures are vertical, striking 104°; top of photographs to north; 46° 58′ 28.6″, 11° 47′ 52.1″). (a) Thin fracture without any apparent offset. (b) Same fracture 1 m further west showing a dextral offset of a thin aplite dyke by ca. 4 cm.

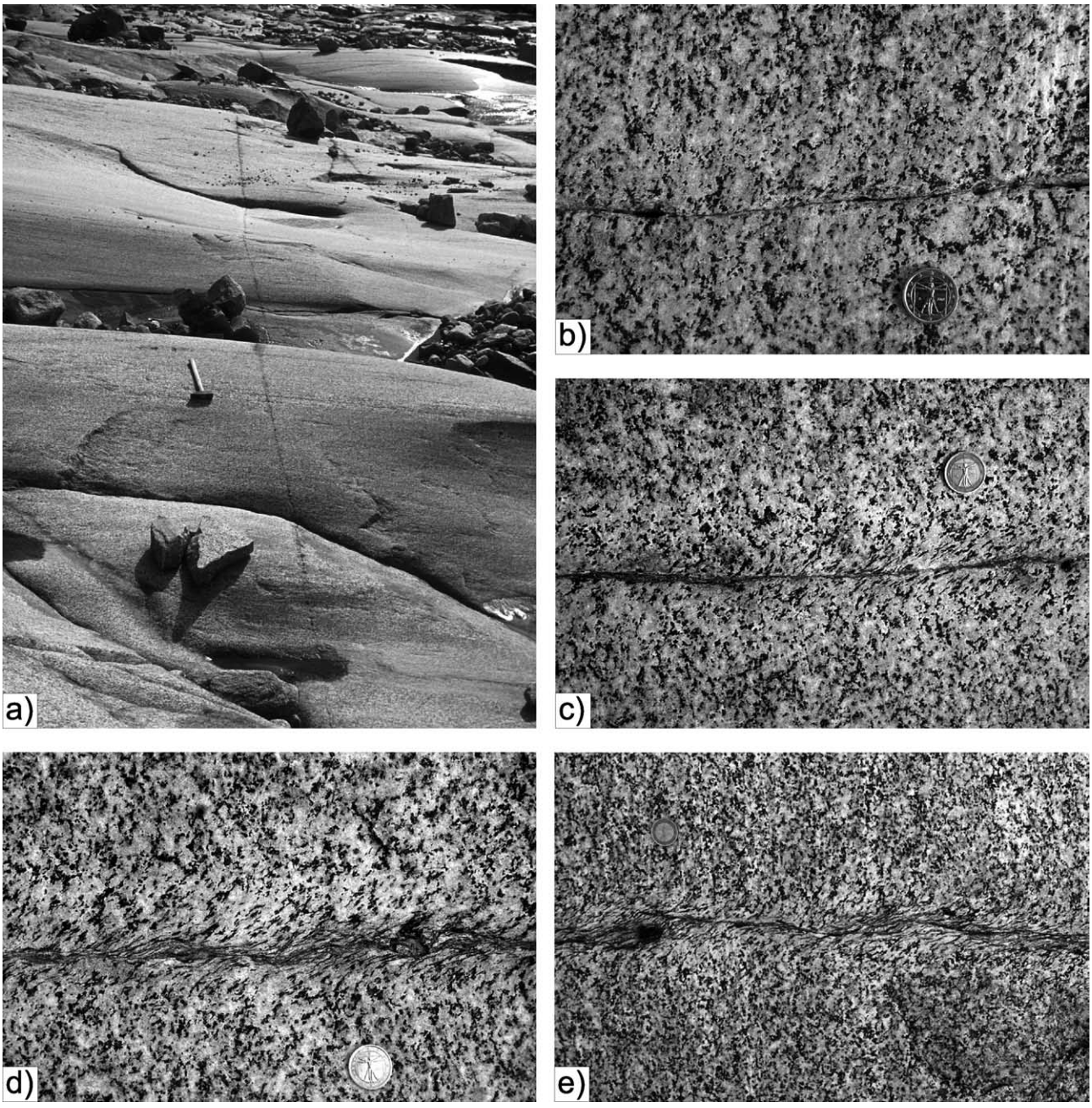

Fig. 4. (a) Single continuous fracture crosscutting otherwise apparently undeformed granodiorite (the fracture is nearly vertical, striking 103°; view looking 100°; 46° 58′ 29.7″, 11° 47′ 52.4″). (b) Close-up of the thin fracture surface marked by enrichment in biotite at the site of the hammer visible in (a). (c) Minor ductile dextral shear reactivation flanking the central biotite-rich fracture, 6 m east of the hammer. Note that the incipient foliation makes an angle near 45° to the trend of the central fracture. (d) Extensive ductile reactivation, with a weak left-stepping SC′ pattern reflecting the initial low-angle en-échelon pattern of brittle fractures, 8 m east of the hammer. (e) Clear left-stepping SC′ pattern reflecting the initial low-angle en-échelon pattern of fractures, 12 m east of the hammer.

ductile shear zones (Fig. 4d and e). The inclined foliation indicates a dextral sense of shear. Where observed, the biotite lineation on fractures is near horizontal and identical to the stretching lineation in the associated ductile shear zones.

Many fractures are segmented with a low-angle, mostly left-stepping, en-échelon geometry, usually with a slight overlap at their terminations (Fig. 5a and b), or terminate in horsetail splay type structures. Locally, single fracture segments several metres in length are connected by linking coplanar damage zones delineated by densely spaced, low-angle, en-échelon fracture arrays. This pattern of low-angle left-stepping primary fractures, developing compressional bridges for dextral shear, is the same as reported for analogue experiments in drained clay and in natural examples by Gamond (1983, 1987). Pennacchioni (2005)

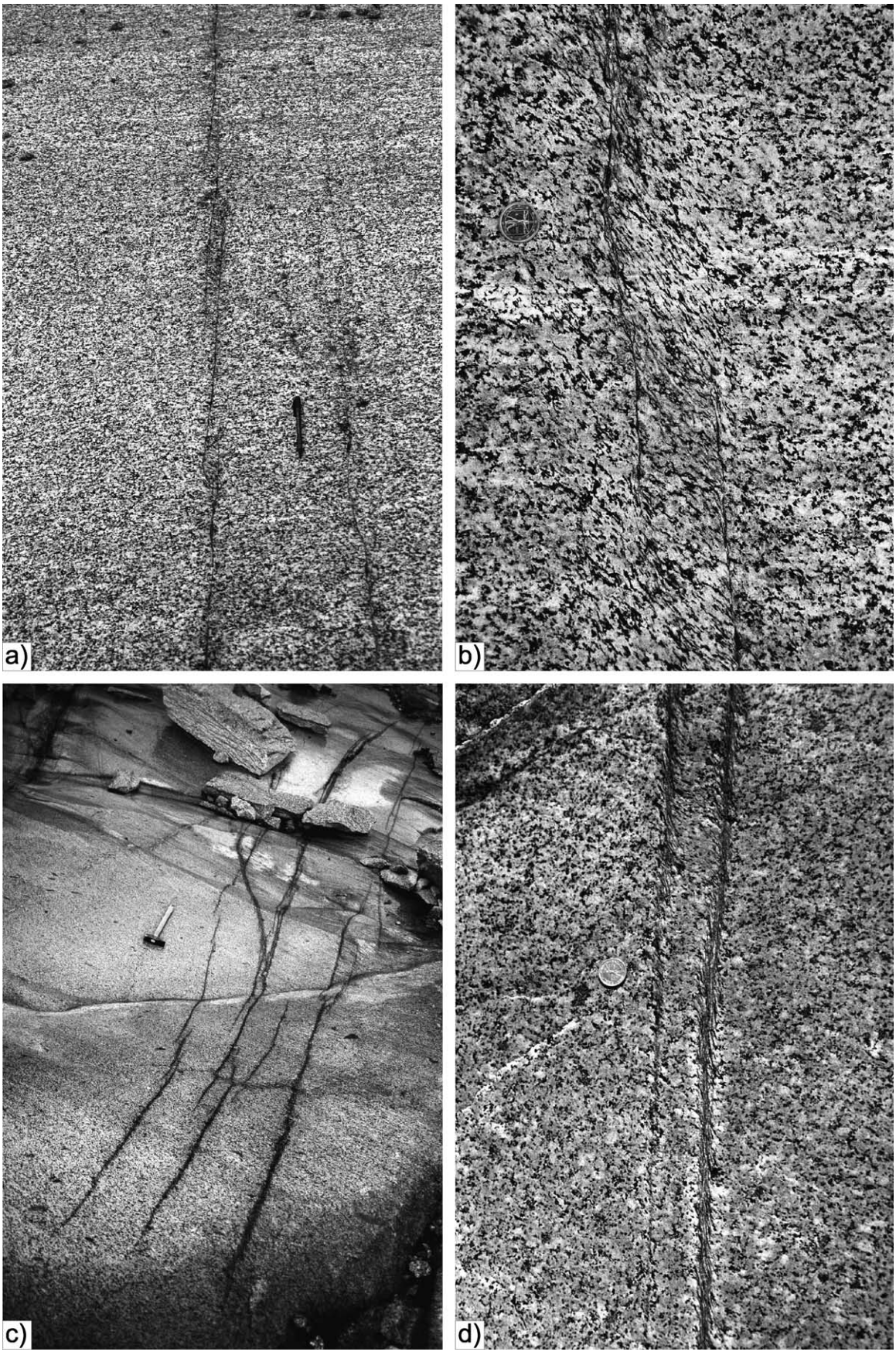
a)
b)
c)
d)

also described such compressional bridges for comparable strike-slip faults in tonalite from the Adamello (Italy). In contrast, Segall and Pollard (1983) reported that stepovers in strike-slip faults developed in granite of the Sierra Nevada (California) are typically dilational.

In the less deformed metagranodiorites, the foliation associated with fractures is exclusively or more intensively developed in the compressional bridges between stepped terminations of en-échelon fractures (Fig. 5a and b). Where the offset on the fractures is small and the strain within the compressional bridges correspondingly rather low, foliation is nearly straight and inclined at ca. 45° to the bounding fracture segments (Fig. 5b).

3.2. Ductile shear zones

The studied area displays all stages of evolution, from incipient ductile reactivation of brittle fractures (Fig. 4a–c) to 'mature' shear zones showing a range of geometries (e.g. Figs. 4d and e and 5c and d). Many of these shear zones remain strongly localized despite the relatively large accommodated strain, with a typical thickness on the order of a few centimetres. This thickness remains approximately constant over the whole length of the shear zone, which can reach several tens of metres (Fig. 5c).

Even in quite advanced stages of ductile shear zone development, the brittle precursor may still be recognized as a straight, narrow, discrete biotite-rich zone in the centre of the foliated zone. Quite commonly, multiple, discrete, and nearly parallel biotite-rich zones are observed on a scale of a few centimetres, leading to a geometry superficially similar to the SC structure originally described by Berthé et al. (1979). In detail, these 'C' planes form a stair-stepped or en-échelon geometry at a small acute angle, reflecting the initial stepped fracture pattern with compressive bridges in the stepovers (Fig. 4e). The geometry is therefore closer to SC′ (Berthé et al., 1979), shear-band (White et al., 1980), or ECC (Platt and Vissers, 1980) structures, with the shear bands at a small synthetic angle to the shear zone boundary. In advanced stages of ductile overprint and broadening, the initial fracture may not be directly visible but the larger scale en-échelon offset is still preserved (Fig. 5c), reflecting the geometry of the brittle precursor (e.g. Fig. 5a). Ductile shear zones developed from overstepped fractures preserve the overstepped geometry to form one type of short-range paired shear zone geometry (Fig. 5d). In the outcrops considered here, the maximum length of these paired zones due to stepover is on the order of 1–2 m.

3.3. Veins and alteration haloes associated with fractures

Pale green epidote-rich ($\pm$garnet$\pm$calcite$\pm$quartz) veins are common along the E–W fractures (Fig. 6a–c). The veins are a few millimetres to (rarely) a few centimetres thick and may be continuous, over distances up to several metres, or discontinuous along the fractures (Fig. 6b). In many examples, a marked bleached zone is developed symmetrically to either side of the vein (Fig. 6a and b). The bleached zones are especially visible on wet outcrop surfaces. A different alteration halo is also present along fractures with a relatively thick filling of biotite. These haloes are typically more coarse-grained than the host granodiorite and show splays of biotite growing randomly away from the central vein (Fig. 6e). The bleached/alteration haloes may remain relatively constant in thickness over most of the fracture/vein length (Fig. 6c and e) or they may show a pinch-and-swell geometry, with significant variation in thickness over short distances along the fracture length (Fig. 6a). In all cases, they maintain an approximately symmetrical geometry about the central fracture or vein. The maximum halo thickness observed is about 50 cm.

3.4. Paired shear zones

The bleached/altered zones developed to either side of the fractures and veins are almost invariably bordered by narrow heterogeneous ductile shear zones (Fig. 6). The spacing of these paired shear zones directly reflects the width of the altered zone, so that the spacing varies both for different zones (e.g. compare Fig. 6b–d) and along the length of a single zone (e.g. Fig. 6a). The relationship between paired shear zones and the alteration haloes is particularly evident where veins are not continuously developed along the fracture plane. In this case, paired shear zones are developed adjacent to the alteration halo flanking the vein but converge to a single shear zone along the fracture trace where the vein and halo are absent.

In general, the bleached/altered zone to either side of the central fracture/vein appears to be very little deformed, with almost no distortion of crosscutting markers (Fig. 7b). Shear is preferentially partitioned onto the flanking shear zones and the central fracture/vein (Fig. 7a and c). However, in some cases a weak foliation may be present between the paired shear zones, continuous with the foliation of bounding shear zones and locally at a high angle to the fracture/shear plane (Fig. 6c and d). In examples where the flanking shear zones have broadened into the adjacent granodiorite, the weakly deformed bleached central zone is typically preserved as a relict within the strongly foliated rock (Fig. 6f).

Fig. 5. (a) Typical left-handed en-échelon offset of discrete fractures (looking west, 46° 58′ 30.3″, 11° 47′ 52.5″). (b) Foliation pattern, clearly outlined by elongate dark biotite clots, marking a ductile compressive bridge between two en-échelon discrete fractures; same outcrop as (a). (c) Left-stepping en-échelon pattern preserved in 'mature' heterogeneous ductile shear zones (looking east, 46° 58′ 23.2″, 11° 47′ 48.6″). (d) Overstepped region of the ductile shear zones, showing the short-range paired pattern, same location as (c).

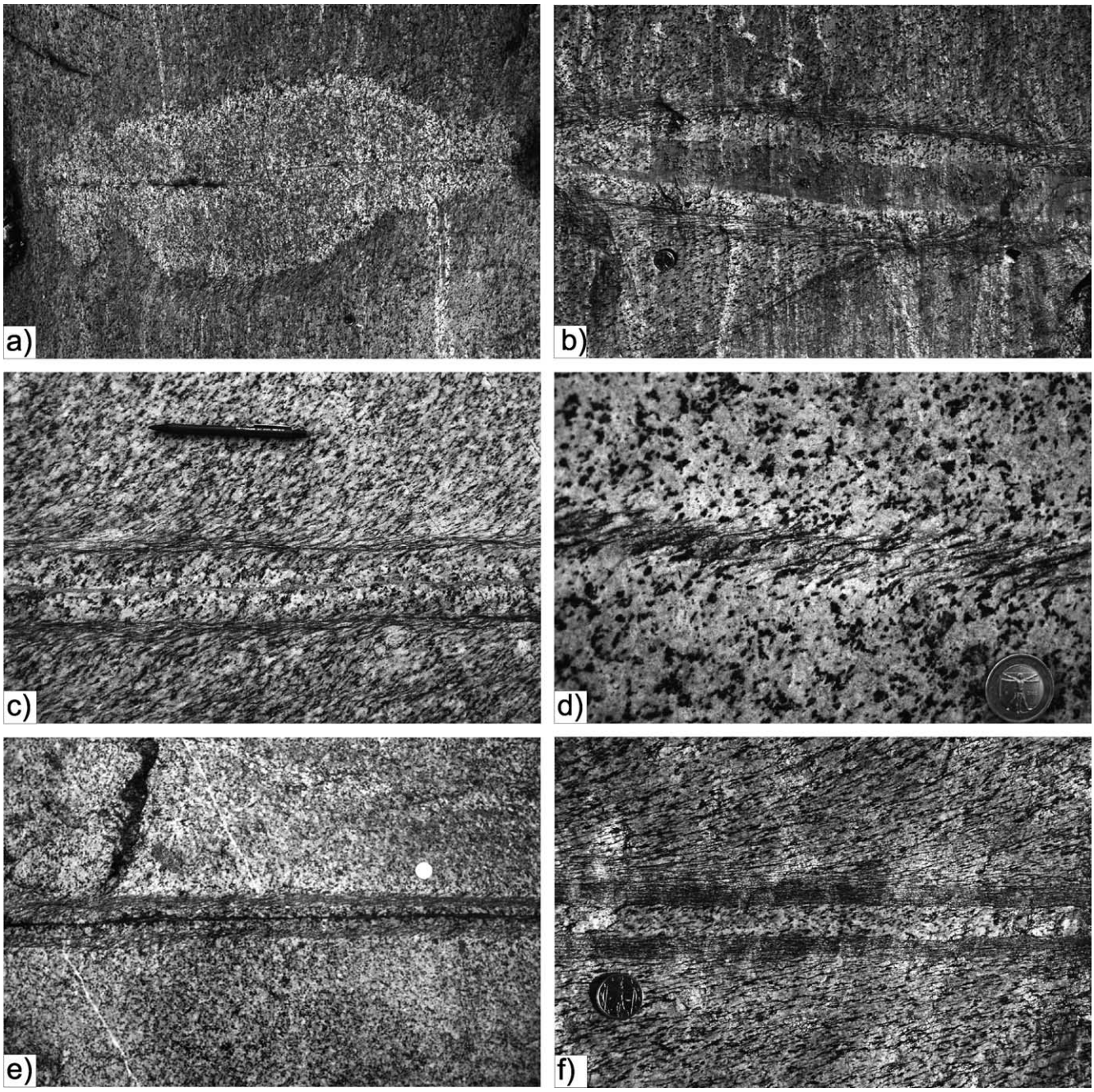

Fig. 6. Veining along fractures, with the development of bleached haloes and flanking paired shear zones. Top of photograph in all cases to the north. (a) Epidote-rich vein along a fracture showing a typical left-stepping compressive bridge and developing a strongly bleached halo approximately symmetric about the central vein. Note also the weakly developed flanking paired shear zones, with the spacing of the shear zones reflecting the variation in width of the bleached zone (46° 58′ 26.9″, 11° 47′ 55.8″). (b) Bleached zone to either side of a central epidote-rich vein, with more strongly developed flanking paired shear zones again varying in spacing with the width of the bleached zone (46° 58′ 34.2″, 11° 47′ 53.6″). (c) Well developed paired shear zone with clear central epidote-rich vein (46° 58′ 23.9″, 11° 47′ 45.7″). (d) Finer scale paired shear zone, without a clearly defined central fracture or vein (46° 58′ 20.3″, 11° 47′ 48.0″). (e) Paired shear zone, with a clear biotite-rich central vein. Total amount of dextral displacement is indicated by the thin aplitic vein. Note the coarse blocky biotite growth away from the central vein into the altered halo and the apparent lack of significant deformation in the halo (46° 58′ 18.8″, 11° 47′ 43.4″). (f) Preservation of a weakly deformed bleached zone as a relict within a broader zone of shearing, with paired zones of more intense shearing adjacent to the altered zone (46° 58′ 26.0″, 11° 47′ 47.9″).

The amount of shear partitioned onto the central fracture/vein apparently depends on its composition (or the composition is changed as the result of shear, e.g. Selverstone et al., 1991; Barnes et al., 2004). Although there are exceptions (see Fig. 10a below), epidote-rich central veins do not usually accommodate much displacement (Fig. 6c), whereas biotite-rich fractures/veins are often highly sheared (Fig. 7a and c).

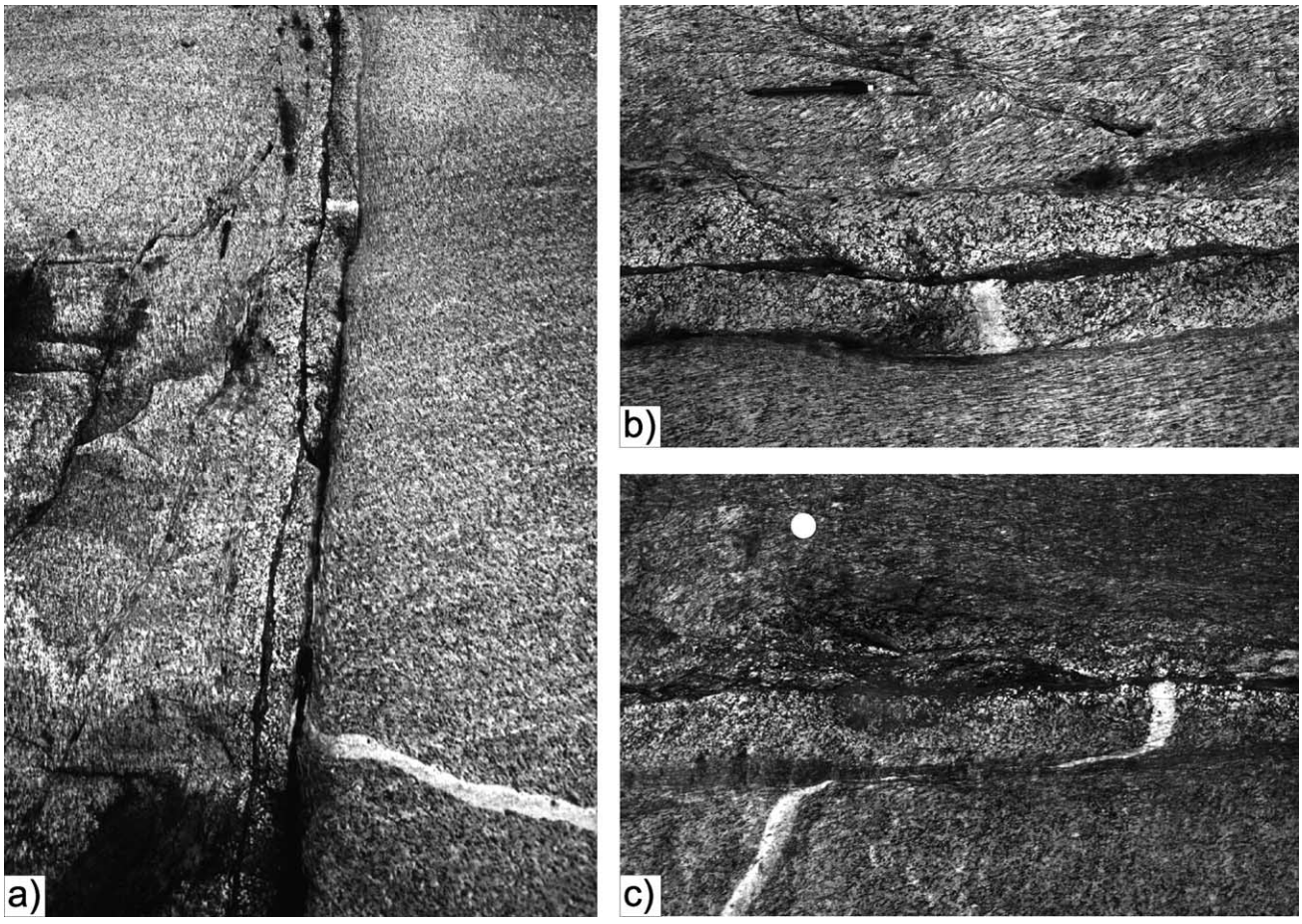

Fig. 7. Partitioning of shear strain between the central fracture/vein, the adjacent bleached halo and the flanking paired shear zones. At least for biotite-rich examples, most displacement occurs on the central fracture, a subordinate amount on the flanking shear zones, and very little in the altered zones to either side of the central fracture. (a) Paired shear zone, looking east (46° 58′ 27.3″, 11° 48′ 01.6″). Note the rapid gradient in shear strain outlined by the aplite dyke on the right side of the bleached zone, and the weak shearing within the bleached zone itself. The aplite dyke is sharply offset across the central reactivated biotite-rich fracture/vein beyond the upper edge of the photograph (and beyond the extent of the outcrop). (b) Close-up of the upper region of (a). Top of photograph is to the north and the pencil for scale is in the same location as in (a). Note the very low shear strain within the bleached halo and the rapid gradient in shear strain into both the flanking shear zone and the central reactivated biotite-rich vein. (c) Nearby paired shear zone, again showing strong ductile shearing within the zone flanking the bleached zone and discrete offset across the central biotite-rich vein. Top of photograph to north (46° 58′ 29.6″, 11° 48′ 03.4″).

Another type of paired shear zones may also develop within the granodiorite at the immediate border to aplite dykes (Fig. 8). One unusual case was observed of paired shear zones that were still symmetrically spaced to either side of an aplite dyke, but occurred at a short distance into the granodiorite (Fig. 8c). Although hardly discernible in the field because of the lack of biotite, these aplite dykes do show an internal shear deformation, but it is far less intense and localized than in the adjacent granodiorite.

4. Microscopic observations

4.1. ‘Undeformed’ metagranodiorites

The metamorphosed magmatic protolith consists of quartz, biotite, plagioclase ± K-feldspar ± muscovite. Allanite is an almost ubiquitous accessory mineral. Under the microscope, all the investigated samples display an extensive metamorphic overprint of the primary minerals and typical deformation microstructures, even though the igneous fabric is macroscopically well preserved.

Quartz occurs as polycrystalline irregular aggregates of coarse grains (several hundred micrometres to a few millimetres in diameter) with grain boundaries that are either stepped, with angles close to 90°, or irregularly serrate to lobate, indicative of fast grain-boundary migration (cf. Urai et al., 1986). Quartz grains do not show optical evidence of internal deformation, except for local weak undulose extinction and coarse deformation bands.

The magmatic biotite (biotite$_1$) is partially to extensively recrystallized, forming decussate to weakly-oriented aggregates of smaller biotite$_2$ (Fig. 9a). It is locally poikilitic to skeletal, with numerous small plagioclase inclusions (ca. 100 μm in diameter). Biotite$_1$ also includes small titanite grains, especially aligned along grain boundaries and

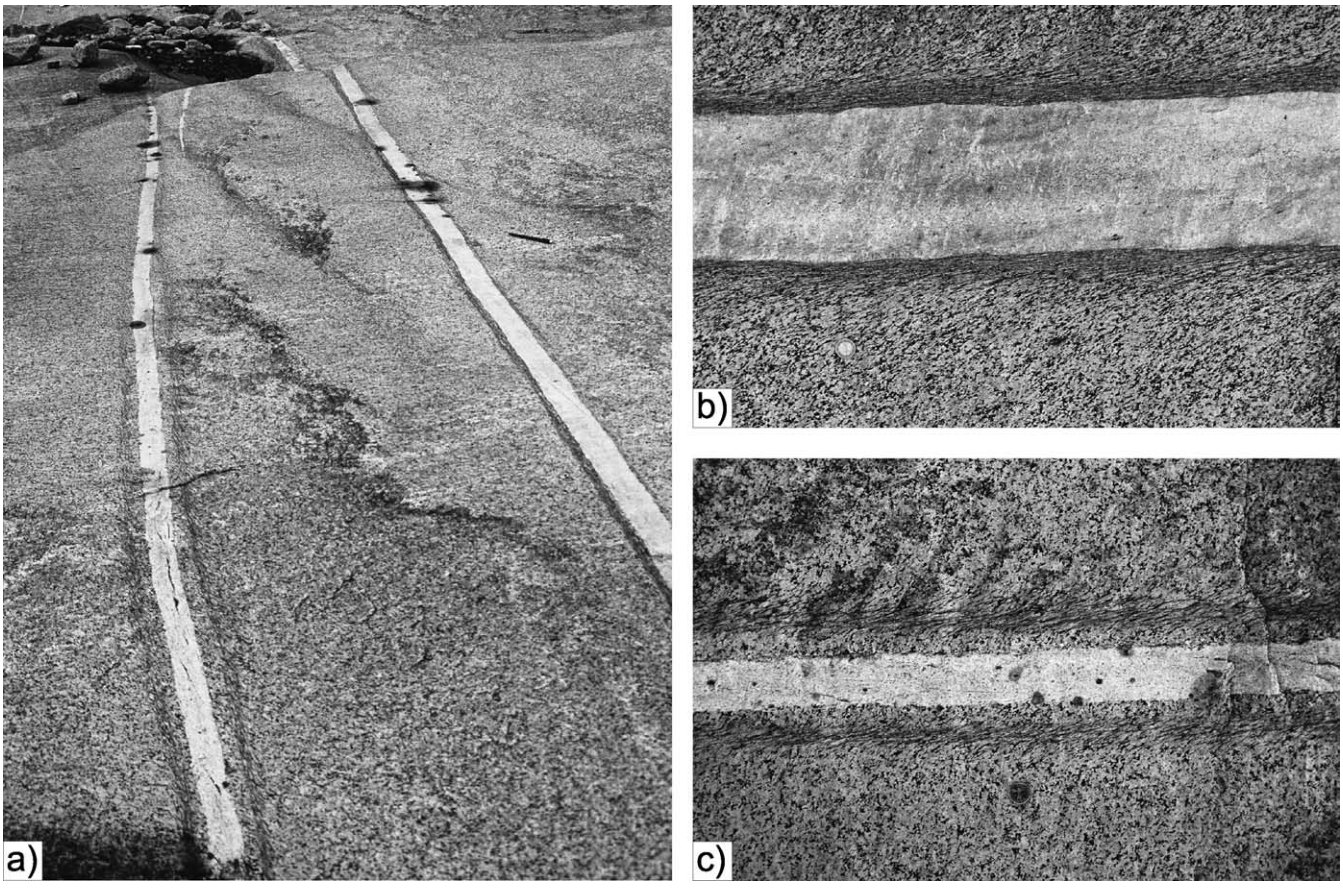

Fig. 8. Shear zones bordering aplite dykes (46° 58′ 26.7″, 11° 48′ 02.9″). (a) Overview of two dykes, looking west, with paired shear zones developed in the adjacent metagranodiorite. (b) The typical relationship, where the shear zones are immediately adjacent to the dyke contact. Top of photograph to north. (c) The atypical case, where the shear zones are symmetrically disposed at a short distance into the adjacent metagranodiorite. Top of photograph to north.

internal deformation features, as well as small rounded zircon grains.

In the best preserved metagranodiorite, plagioclase$_1$ occurs as prismatic crystals (up to several millimetres in length) typically with disseminated fine-grained inclusions of epidote ± white mica ± biotite (Fig. 9b). Epidote inclusions occur as small granules (less than a few tens of micrometres in diameter) and disoriented elongate crystals (a few hundreds of micrometres in length). Plagioclase$_1$ is locally recrystallized to an aggregate of polygonal grains of plagioclase$_2$ ± quartz. Some of these recrystallized aggregates still contain abundant epidote ± white mica ± biotite inclusions, whereas other aggregates are almost inclusion-free. Some small plagioclase grains within the recrystallized aggregates contain abundant tiny inclusions of quartz that locally show the typical vermicular shape of myrmekitic intergrowth.

K-feldspar distribution has been studied both in stained thin sections (Müller, 1967; section 3.522, pp. 164–167) and from SEM back scattered electron images. It is present in lesser amounts and as smaller grains (less than a few hundred micrometres in diameter) than plagioclase. It has been mainly observed within the polymineralic, relatively fine-grained aggregates of dominant plagioclase.

Prismatic crystals of magmatic allanite are well preserved, with only a thin rim of epitaxial epidote. Garnet is a minor component, occurring as idioblastic grains generally <250 μm in diameter and with a dusty finely poikilitic core. Garnet is associated with both the feldspar- and biotite-rich domains and locally forms a discontinuous coronitic rim at biotite–plagioclase grain boundaries.

Fine-grained granitoids have a similar mineral assemblage and microstructure, the only significant difference being the smaller average grain size. Aplite dykes are composed of quartz, K-feldspar, plagioclase and muscovite.

4.2. Precursor fractures

Few fractures could be observed directly in thin sections because samples tend to preferentially split along these pre-existing planes of weakness. Knife-sharp fractures are always perfectly sealed, without preserved larger scale porosity, and there is no microstructural evidence for cataclasis. Fractures are outlined by newly grown quartz, biotite, epidote and plagioclase. Biotite is (greenish) brown in colour. It is usually oriented approximately parallel to the fracture boundary. However, in some cases it is obliquely oriented and appears to join originally adjacent points on

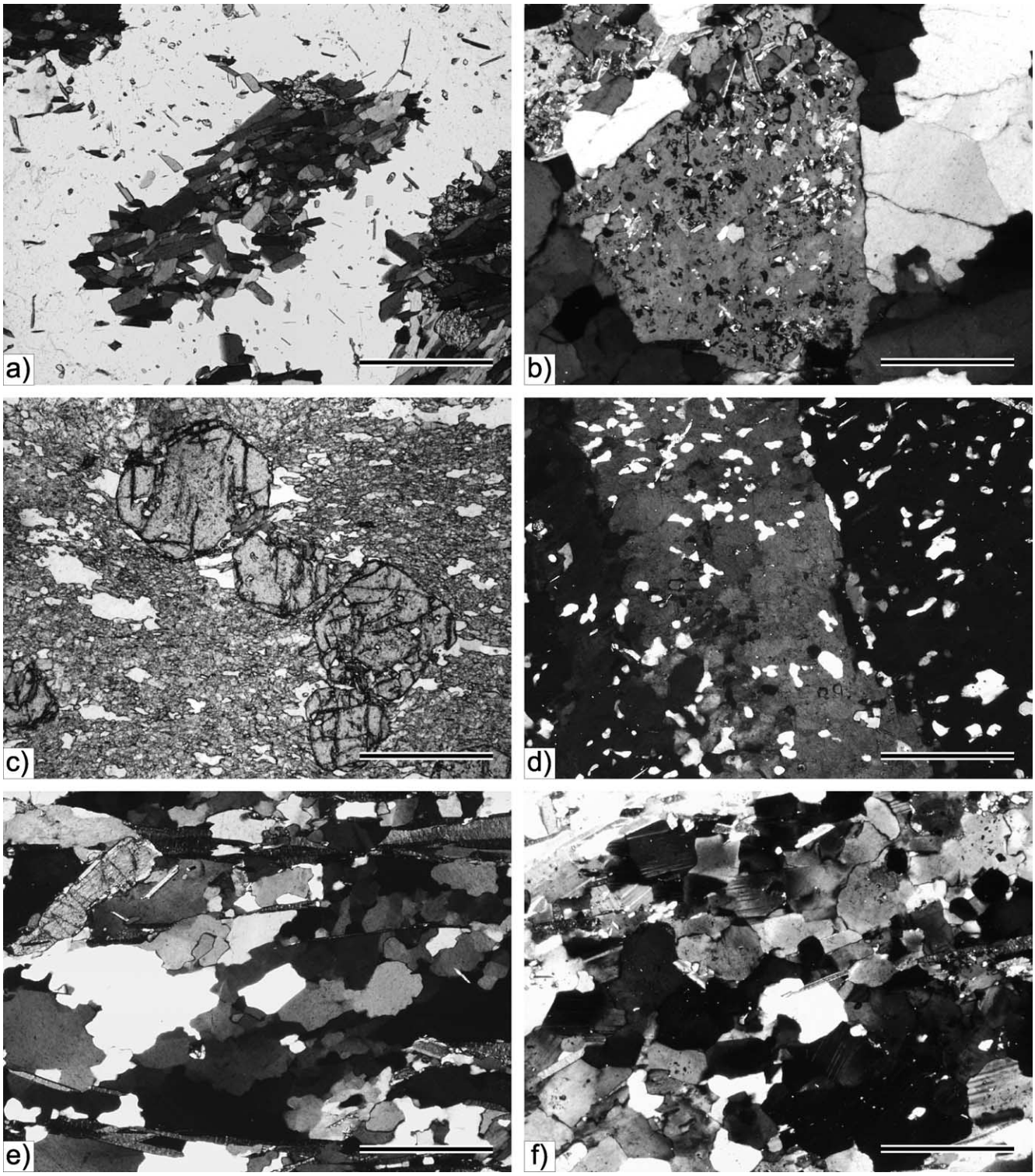

Fig. 9. Optical microstructures. (a) Biotite$_1$ site within an alteration halo, slightly elongated parallel to the weak foliation (approximately NE–SW in the photograph) and showing complete replacement by an aggregate of decussate biotite$_2$ and titanite. Biotite$_2$ is weakly aligned subparallel to the shear plane of adjacent shear zones. Plane polarized light. Such biotite microstructures are also typical of the undeformed metagranodiorite outside the haloes and shear zones. (b) Magmatic saussuritic plagioclase rich in small inclusions of epidote – white mica $\pm$ biotite, which is typical of the undeformed granodiorite outside the bleached haloes. Crossed polars. (c) Garnet idioblasts in a deformed epidote-rich central vein flanked to either side by an alteration halo and paired shear zones. The light-coloured quartz locally forms pressure shadows on the garnet. Plane polarized light. (d) Characteristic poikilitic plagioclase porphyroblasts within bleached haloes, rich in irregular quartz inclusions. Crossed polars. (e) Coarse grained dynamically recrystallized quartz within a shear zone developed by reactivation of a central vein. The lobate to serrated boundaries are typical of fast grain boundary migration recrystallization. The shape fabric is oblique to the subhorizontal mylonitic foliation, outlined by aligned biotite, and is consistent with the dextral shear sense. Crossed polars. (f) Granoblastic aggregate of recrystallized plagioclase$_2$ in the transition zone from alteration halo to flanking shear zone. Crossed polars. Scale bar is 500 μm in all photographs.

either side of the fracture. The offset on unreactivated fractures is small to non-existent, as can be seen by matching individual mineral grains or aggregates across fractures.

An important observation is that the plagioclase grains immediately adjacent to the fractures have a distinctly different internal aspect compared with the 'saussuritic' plagioclase grains typical of the metagranodiorite protolith, although the grain size and shape are comparable. These characteristic plagioclase grains are free of epidote inclusions, and contain little or no white mica or biotite. Instead they are rich in quartz inclusions, commonly showing vermicular intergrowths. This type of plagioclase is also characteristic of the bleached haloes that can develop adjacent to fractures, as described in detail below.

4.3. Veins

Undeformed veins developed along the EW fractures mainly consist of epidote and minor quartz. Garnet, biotite and calcite may be either minor or abundant components in different veins. Epidote forms columnar crystals, several millimetres long, with a preferred orientation orthogonal to vein walls, intergrown with quartz grains. There is no evidence of antitaxial/syntaxial growth or of stretched crystals. Epidote shows internal zoning and is rich in primary solid (quartz) and fluid inclusions.

Sheared veins consist of recrystallized, fine-grained (tens of micrometres) epidote and locally abundant poikilitic (mainly quartz inclusions) garnet idioblasts, <1 mm in diameter, which overgrow the foliation (Figs. 9c and 10a). The local presence of quartz pressure shadows around garnet suggests a syn- to late-kinematic growth (Fig. 9c).

4.4. Alteration haloes

The rock domains between paired shear zones and the central veins show little evidence of deformation (Fig. 7). However, although not always evident macroscopically, under the microscope it can be seen that there is usually strong localized shear reactivation of the vein and the immediately adjacent halo (usually over a thickness of a few millimetres). In the halo close to the central vein, quartz and (to a lesser extent) plagioclase show healed microfractures and grain boundaries decorated by small grains of epidote.

The main differences between the little deformed part of the halo and the typical weakly deformed metagranodiorite are: (1) some haloes contain relatively large amounts of calcite, which is rare in the metagranodiorites, and (2) the plagioclase has a distinctive microstructure. Plagioclase occurs as large poikilitic porphyroblasts up to several millimetres in size, which are rich in inclusions of quartz (tens to a few hundreds of micrometres) $\pm$ biotite (in randomly oriented acicular lamellae smaller than the biotite outside) $\pm$ calcite, but without the saussuritic aggregates typical of plagioclase grains in the metagranodiorite (cf. Fig. 9b). Quartz inclusions commonly have an irregular shape that is locally transitional to a vermicular microstructure typical of quartz–plagioclase myrmekitic intergrowths (Fig. 9d). Groups of adjacent quartz inclusions display an identical CPO, which is evident under crossed polars with the gypsum plate inserted; this is also characteristic of myrmekites. The plagioclase locally contains isolated corroded relicts of K-feldspar showing an irregular shape (Fig. 10b and c) that is sporadically controlled by the cleavage orientation of the host plagioclase. Different K-feldspar relicts within a single plagioclase porphyroblast have an identical crystallographic orientation. The quartz inclusion-rich portions of the plagioclase may have a turbid appearance in thin section due to the presence of abundant ultrafine solid and fluid inclusions. Most plagioclase porphyroclasts show an irregular optical extinction, reflecting a patchy compositional zoning in the range of An_{15}–An_{25}. The highest Ca compositions are in some cases spatially associated with more inclusion-rich domains. Overall, these features suggest that the poikilitic plagioclase originated as myrmekitic aggregates replacing primary K-feldspar. However, myrmekites are not observed in contact with the relict K-feldspar enclosed within the plagioclase. Most myrmekitic plagioclase is simply in contact with other non-myrmekitic plagioclase. Peripheral zones of the plagioclase porphyroblasts have overgrown biotite, which is still preserved as corroded relicts oriented parallel to the weak foliation in the surrounding matrix.

Particularly within the transitions to the more strongly sheared central vein and the flanking paired shear zones, the plagioclase from the alteration halo can show a progressive recrystallization to polymineralic plagioclase$_2$ $\pm$ quartz aggregates (Figs. 9f and 10c). The microstructure of quartz and biotite in the haloes is basically similar to that already described for the weakly deformed metagranodiorites (Section 4.1).

4.5. Paired and single shear zones

The microstructural characteristics of paired and single shear zones are quite similar and will be described together, highlighting specific differences. As observed directly in outcrop, there is a very strong gradient in strain and foliation development at the rim of all shear zones. In the outer low strain portions, aggregates of brown biotite pseudomorph the original coarse magmatic biotite (Fig. 9a). Traversing into the shear zones, the biotite aggregates are progressively rotated and stretched; these elongate dark lenses largely define the observed sigmoidal foliation (Figs. 4–8). The biotite is clearly stable during this deformation and shows no evidence of retrogression or fragmentation. Within the elongate aggregates, individual biotite grains are either disoriented, forming decussate fabrics, or roughly oriented parallel to the biotite aggregate elongation. In the shear zones, biotite is commonly associated with small idiomorphic garnet. Plagioclase is extensively replaced by

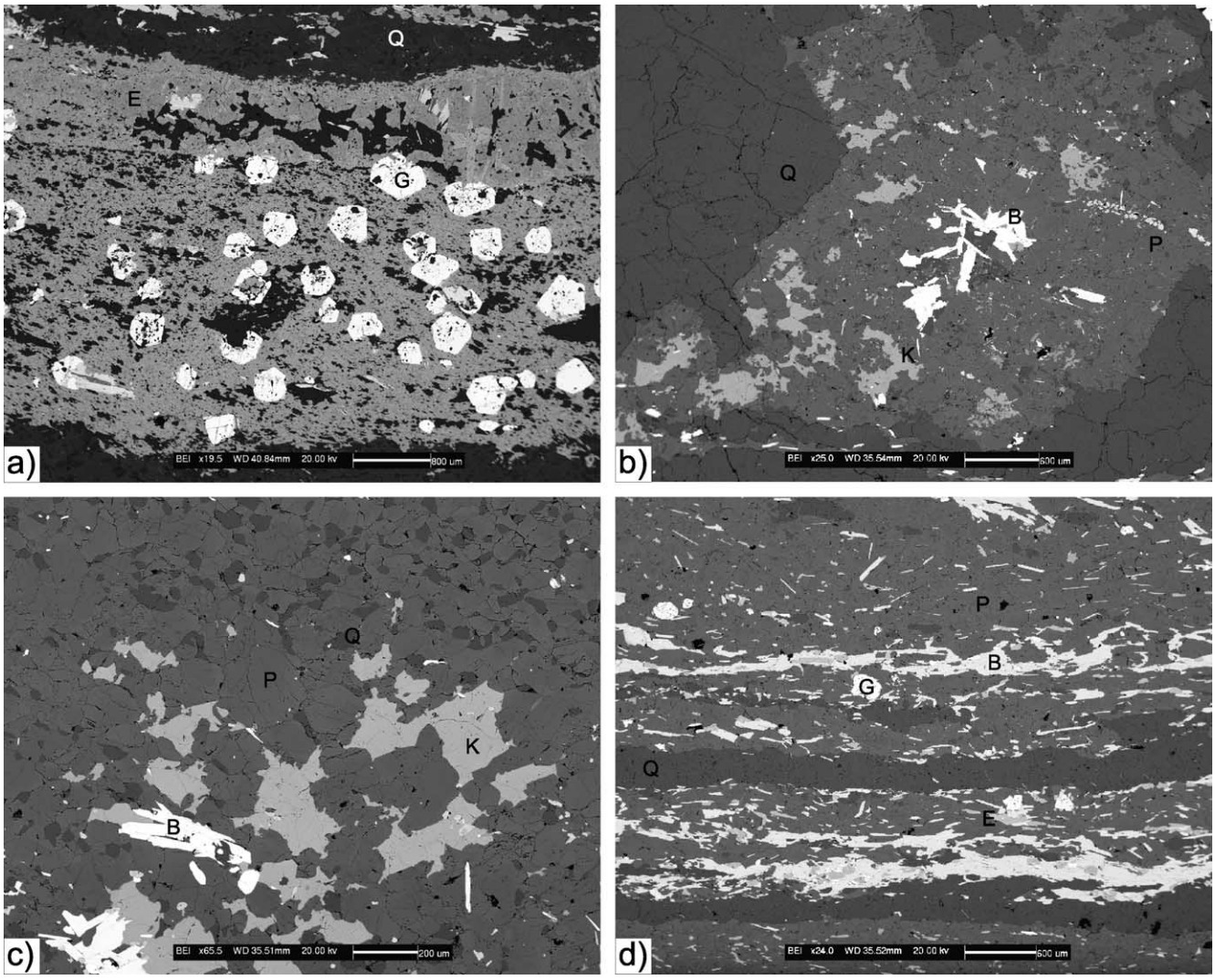

Fig. 10. SEM backscatter images. (a) Sheared epidote-rich vein central to an alteration halo with an adjacent shear zone pair. The relict primary epidote (E) and quartz (Q) vein assemblage is preserved in the upper part of the vein. Idioblastic garnet (G) mainly grows in the lower strongly sheared part, which consists of a fine-grained aggregate of epidote and quartz outlining a foliation subparallel to the vein boundary. (b) Irregular K-feldspar relicts (K) within an aggregate of dominant plagioclase$_2$ (P). The white platy mineral is biotite (B) and the large dark domains are quartz (Q). (c) Irregular K-feldspar relicts (K) within plagioclase (P), recrystallized in the upper part to a finer-grained aggregate of plagioclase$_2$ (light grey) and quartz (Q, dark grey). (d) Compositional layering in the central mylonitic part of a shear zone flanking a bleached halo. The layering consists of quartz ribbons (Q), biotite$_2$-rich folia (B) and domains of fine-grained recrystallized plagioclase$_2$ (P) $\pm$ quartz, including scattered small prismatic epidote grains (E). The bright equant grains are garnet (G).

recrystallized aggregates of polygonal plagioclase$_2$ $\pm$ quartz $\pm$ oriented epidote–white mica–biotite (Fig. 9f), but still contains scattered relicts of the earlier poikilitic plagioclase in the transition zone to 'undeformed' metagranodiorite. The mean grain size of plagioclase$_2$ is <200 μm. Mica grains are either scattered in the matrix or, in the case of white mica, form discontinuous layers parallel to the foliation. Quartz aggregates are elongated parallel to the new foliation and dynamically recrystallized, with irregular boundaries typical of grain boundary migration. The recrystallized grain size of quartz is large (on the order of hundreds of micrometres).

Mylonites forming the core of single and paired shear zones are relatively fine grained and display a variably developed but distinct compositional layering consisting of alternating pure quartz ribbons, plagioclase-rich domains and biotite-rich domains (Fig. 10d). The grain size of quartz is finer and less heterogeneous than in the metagranodiorite and low strain portions of the shear zones, but it is still relatively large (hundreds of micrometres). Quartz aggregates have a clear crystallographic preferred orientation (CPO), reflected in a marked gypsum plate effect. Quartz grains in one-grain-thick ribbons confined between mica layers have a blocky shape. Otherwise, the majority of quartz grains are irregularly serrated, typically asymmetric, and oriented oblique to the main foliation (Fig. 9e), indicating the sense of shear. The quartz microstructure suggests synkinematic recrystallization by fast grain boundary migration. Plagioclase occurs in granoblastic aggregates of equant to slightly elongate grains. Grain

shapes are polygonal to serrated. Minor quartz is present, typically at triple grains junctions of plagioclase within the recrystallized plagioclase-rich aggregate. In some samples of single shear zones, there is a clear relative enrichment of K-feldspar within the high strain part of the shear zone. K-feldspar forms large elongated grains that include biotite lamellae well aligned with the mylonitic foliation. K-feldspar grains locally show very small myrmekitic lobes of vermicular quartz and plagioclase. Single shear zones nucleated on precursor brittle fractures still commonly preserve a distinguishable thin central layer of very fine-grained biotite, plagioclase, quartz and epidote, outlining the initial reactivated fracture.

In thin section, paired shear zones in the metagranodiorite immediately adjacent to aplite veins are less clear-cut than they appear in the field. The aplite dykes themselves are also quite strongly deformed, with a marked foliation defined by elongate quartz and feldspar. There is, however, minor refraction in the orientation of the foliation, indicating less shear in the centre of the aplite dyke compared with the rims. Similar to the bleached halo examples, the paired shear zones therefore apparently develop where there is a sharp or rapidly gradational change in material properties and rheology between a stronger core and a weaker external matrix.

5. Discussion

The progressive spatial development of more distributed ductile shear zones from discrete brittle fractures can be directly observed in continuous glacially-polished exposures of otherwise weakly deformed metagranodiorites. If these spatial variations provide a distributed snapshot of the temporal variation within a single zone, then the progressive development of strongly localized, heterogeneous shear zones can be established from these field observations.

The geometry of the initial fractures and the degree of fluid–rock interaction along and adjacent to the fractures has controlled the geometric pattern of the subsequent ductile shear zones. Amphibolite facies metamorphic conditions during ductile reactivation of fractures are indicated by: (1) the growth of biotite and garnet in both fractures and shear zones; (2) the microstructure of quartz indicating dynamic recrystallization dominated by fast grain boundary migration; and (3) the development and recrystallization of myrmekitic plagioclase of oligoclase composition during shearing. Even when reactivation is restricted to the discrete narrow zone of the initial fracture (e.g. Fig. 3b), strain is accommodated at the grain scale dominantly by crystal plastic mechanisms (Segall and Pollard, 1983; Simpson, 1985, 1986; Segall and Simpson, 1986), as indicated by strong crystallographic preferred orientation, oblique elongate grain fabrics and dynamic recrystallization of quartz and plagioclase. The relation between discrete reactivated fractures and ductile compressive bridges establishes that both components were active simultaneously. The displacement rates on the discrete reactivated fractures were sufficiently slow for strain to be accommodated within the bridging zones in a distributed and ductile manner.

Although fracture reactivation and the ductile compressive bridges are clearly coeval, the timing of initial fracturing cannot be determined with certainty. Most initial fractures are dilatant joints, without shear offset, and could have developed during cooling of the original Hercynian pluton (cf. Pennacchioni, 2005). Hercynian initiation and Alpine reactivation would then be two completely separate events. As shown in Fig. 8c, one example has been found of an aplite dyke with paired shear zones developed at a constant distance from the dyke rim. A possible explanation would be that the aplite dyke intruded along an existing fracture/vein that had already developed an adjacent bleached halo (R. Rutland, pers. comm., 2004). In this case, the fracturing, fluid–rock interaction (with halo formation), and aplite dyke intrusion would all be Hercynian and only the flanking paired shear zone formation would be of Alpine age.

However, there is also good evidence that both initial fracturing and reactivation actually occurred under a similar kinematic regime, because: (1) the low-angle en-échelon left-stepping patterns observed (Fig. 5a) suggest a dextral component during fracturing, the same as the subsequent ductile reactivation, and (2) low-strain foliations, e.g. in incipient shear zones adjacent to fractures (Fig. 4c) or in the transition to little deformed metagranodiorite (Figs. 4d, 5b and d and 6), are oriented at angles near 45° to the fracture/shear plane and therefore in the ideal orientation for simple shear zone formation. Rare examples have also been found of reactivated straight fractures offsetting ductile shear zones and of bleached haloes overprinting the sigmoidal foliation of ductile shear zones. Fracturing, associated fluid–rock interaction, and ductile shear localization on precursor fractures therefore appears to be broadly coeval, although varying locally in space and time.

Some ductile shear zones developed from en-échelon initial fracture sets show a geometry similar to that described as C′ structure (Berthé et al., 1979), shear bands (White et al., 1980), or ECC (Platt and Vissers, 1980) (Fig. 4e). However, the origin is quite different. Such shear-band structures were previously envisaged as developing late in the shear zone history as the result of instability in the extending, strongly anisotropic mylonitic foliation (i.e. a form of asymmetric foliation boudinage). In the current model, the low-angle stepped en-échelon geometry is already determined by the brittle precursor, prior to significant subsequent ductile overprint. As foliation becomes more intense and distributed, late-stage shear band structures may still develop as previously envisaged in the strongly foliated zones.

Shear zones, both in the area considered in detail here

and in other regions ranging from amphibolite to eclogite facies (Fig. 2), may show a characteristic paired geometry. Some examples of short-range pairing are simply related to overstepping of ductile shear zones controlled by the original stepped brittle fracture geometry (Fig. 5d). However, the length of such overstepping seldom exceeds 1–2 m. More persistent paired zones are a direct result of fluid–rock interaction along the initial fracture. This can lead to the development of an alteration halo to either side, with subsequent ductile shear zone development occurring on the borders of this altered zone to produce the characteristic paired pattern. Alteration involves the growth of large new plagioclase grains containing vermicular quartz inclusions (Fig. 9d). Based on the distribution of subsequent deformation, the altered zones were apparently rheologically strong and thus remained little deformed during subsequent shearing (Fig. 7). Shear is concentrated on the central fracture or vein and at the rim of the altered zone. Other paired shear zones develop near the rims of aplite dykes.

The localization of shear strain on the borders of both the bleached zones and of the aplite dykes implies that these border regions are rheologically weaker than both the central zone and the adjacent protolith. As noted by Segall and Simpson (1986), this remains a major unresolved problem. They suggested "that enhanced ductility of the wall rock may result from chemical alteration and/or hydrolytic weakening caused by aqueous fluids in the earlier dilatant fracture". However, in the current example the introduction or withdrawal of fluid along the central vein has in most cases produced an adjacent halo of fluid–rock interaction that is markedly harder than the initial protolith. It is also clear that fluid–rock interaction and shearing must be sequential for any individual paired shear zone, because the sheared fabric developed at the final boundary position of the bleached zone and was not overprinted by an advancing reaction front. Indeed it is possible that initial dilatant fracturing (i.e. jointing) and fluid–rock interaction occurred during cooling of the Hercynian pluton and that only the ductile reactivation of the central fracture/vein and bleached zone boundary reflects Alpine deformation. In their examples from Sierra Nevada, California, and Roses, northeast Spain, Segall and Simpson (1986) proposed that brittle faulting occurred in intact protolith synchronously with ductile flanking shear zone development in more mature zones. Spreading of deformation to progressively embrace more of the plutonic body would require such a scenario. However, this would also require the shear stress acting on adjacent and parallel mature and incipient zones to be approximately the same (Cobbold, 1977b), which would imply that the reaction front to the progressively widening alteration halo was not weak until it had ceased to advance. A mechanism of weakening during reaction would therefore not be appropriate.

The bulk background strain in the metagranodiorite is much lower than in the shear zones but it is not zero. In fact, there is a tendency to underestimate this background strain in the field because the solid state deformation must first overcome the strong ca. NS striking magmatic fabric. Because the magmatic and solid state fabrics are almost perpendicular, initial solid state deformation leads to a reduction in elongation of the mafic enclaves and biotite clots, so that a rather equant macroscopic fabric can actually represent a quite significant tectonic overprint. A model invoking flanking structures (Grasemann and Stüwe, 2001; Passchier, 2001; Grasemann et al., 2003) developed to either side of a crosscutting rheological discontinuity (e.g. a fracture or a dyke) within an otherwise more homogeneously shearing rock body may therefore be appropriate. Such a flanking structure model could explain the spatial distribution, with localization occurring at rheological boundaries. However, without some positive feedback between strain (or strain rate) and rheology, it could not explain the magnitude of the strain in the localized zones, because the background strain in the metagranodiorite is apparently insufficient compared with that necessary for well-developed flanking structures (cf. Exner et al., 2004).

6. Conclusions

Shear zone development under amphibolite facies conditions in the initially little deformed and homogeneous metagranodiorite followed the sequence: (1) initial brittle fracture; (2) fluid–rock interaction and development of a bleached halo of variable thickness, symmetric about the central vein; and (3) ductile shear zone development on the borders of the bleached band. The degree and geometry of the fluid–rock interaction determined the geometry of the ductile shear zones. Where no halo was present, single ductile shear zones were developed during subsequent reactivation, with the fracture preserved as a biotite-rich straight suture in the centre of the shear zone. Where a halo was developed, reactivation led to a paired geometry as the ductile shearing concentrated on the central fracture/vein and the rims of the halo. Such characteristic paired shear zones have also been observed in other regions and metamorphic environments. The common feature is the relationship between initial fracture, fluid–rock interaction along the fracture and with the adjacent protolith, and the subsequent localization of ductile shear on the central fracture and the rims of the alteration halo. Heterogeneous shear zones are developed not only on weak precursor fractures but also flanking more competent bleached haloes and aplite dykes. Localization therefore occurred at rheological boundaries rather than in bands of weaker material.

Acknowledgements

Mike Williams is thanked for a thorough and helpful

review. The generous help of the guardian of the Chemnitzer Hütte (Rifugio Porro), Roland Gruber, is also gratefully acknowledged. NM received financial support from ETH research project TH 0-20998-02 and GP was funded by the University of Padova (fondi quota ex 60%).

References

Arbaret, L., Burg, J.P., 2003. Complex flow in lowest crustal, anastomosing mylonites: strain gradients in a Kohistan gabbro, northern Pakistan. Journal of Geophysical Research-Solid Earth 108, art. no. 2467.

Barnes, J.D., Selverstone, J., Sharp, Z.D., 2004. Interactions between serpentinite devolatilization, metasomatism and strike-slip strain localization during deep-crustal shearing in the Eastern Alps. Journal of Metamorphic Geology 22, 283–300.

Berthé, D., Choukroune, P., Jegouzo, P., 1979. Orthogneiss, mylonite and non-coaxial deformation of granites: the example of the South Armorican Shear Zone. Journal of Structural Geology 1, 31–42.

Bestmann, M., Kunze, K., Matthews, A., 2000. Evolution of a calcite marble shear zone complex on Thassos Island, Greece: microstructural and textural fabrics and their kinematic significance. Journal of Structural Geology 22, 1789–1807.

von Blanckenburg, F., Villa, I.M., Baur, H., Morteani, G., Steiger, R.H., 1989. Time calibration of a PT-path from the western Tauern Window, Eastern Alps: the problem of closure temperatures. Contributions to Mineralogy and Petrology 101, 1–11.

Bowden, P.B., 1970. A criterion for inhomogeneous plastic deformation. Philosophical Magazine (Series 8) 22, 455–462.

Brunsmann, A., Franz, G., Erzinger, J., Landwehr, D., 2000. Zoisite- and clinozoisite-segregations in metabasites (Tauern Window, Austria) as evidence for high-pressure fluid–rock interaction. Journal of Metamorphic Geology 18, 1–21.

Burg, J.P., Laurent, P., 1978. Strain analysis of a shear-zone in a granodiorite. Tectonophysics 47, 15–42.

Carreras, J., Garcia Celma, A., 1982. Quartz C-axis fabric variation at the margins of a shear zone developed in schists from Cap de Creus (Spain). Acta Geològica Hispànica 17, 137–149.

Casey, M., 1980. Mechanics of shear zones in isotropic dilatant materials. Journal of Structural Geology 2, 143–147.

Cesare, B., Poletti, E., Boiron, M.C., Cathelineau, M., 2001. Alpine metamorphism and veining in the Zentralgneis Complex of the SW Tauern Window: a model of fluid–rock interactions based on fluid inclusions. Tectonophysics 336, 121–136.

Christiansen, P.P., Pollard, D.D., 1997. Nucleation, growth and structural development of mylonitic shear zones in granitic rock. Journal of Structural Geology 19, 1159–1172.

Cobbold, P., 1977a. Description and origin of banded deformation structures. I. Regional strain, local perturbations, and deformation bands. Canadian Journal of Earth Sciences 14, 1721–1731.

Cobbold, P., 1977b. Description and origin of banded deformation structures. II. Rheology and the growth of banded perturbations. Canadian Journal of Earth Sciences 14, 2510–2523.

De Vecchi, G.P., Mezzacasa, G., 1986. The Pennine basement and cover units in the Mesule group (southwestern Tauern window). Memorie di Scienze Geologiche 38, 365–392.

Dutruge, G., Burg, J.P., Lapierre, J., Vigneresse, J.L., 1995. Shear strain analysis and periodicity within shear gradients of metagranite shear zones. Journal of Structural Geology 17, 819–830.

Exner, U., Mancktelow, N.S., Grasemann, B., 2004. Progressive development of s-type flanking folds in simple shear. Journal of Structural Geology 26, 2191–2201.

Finger, F., Frasl, G., Haunschmid, B., Lettner, H., von Quadt, A., Schermaier, A., Schindlmayr, A.O., Steyrer, H.P., 1993. The Zentralgneise of the Tauern Window (Eastern Alps): insight into an Intra-Alpine Variscan batholith, in: von Raumer, J.F., Neubauer, F. (Eds.), Pre-Mesozoic Geology in the Alps. Springer-Verlag, Berlin, pp. 375–391.

Finger, F., Roberts, M.P., Haunschmid, B., Schermaier, A., Steyrer, H.P., 1997. Variscan granitoids of central Europe: their typology, potential sources and tectonothermal relations. Mineralogy and Petrology 61, 67–96.

Friedrichsen, H., Morteani, G., 1979. Oxygen and hydrogen isotope studies on minerals from alpine fissures and their gneissic host rocks, western Tauern window (Austria). Contributions to Mineralogy and Petrology 70, 149–152.

Fügenschuh, B., Seward, D., Mancktelow, N., 1997. Exhumation in a convergent orogen: the western Tauern Window. Terra Nova 9, 213–217.

Gamond, J.F., 1983. Displacement features associated with fault zones: a comparison between observed examples and experimental models. Journal of Structural Geology 5, 33–45.

Gamond, J.F., 1987. Bridge structures as sense of displacement criteria in brittle fault zones. Journal of Structural Geology 9, 609–620.

Gilotti, J.A., Kumpulainen, R., 1986. Strain softening induced ductile flow in the Särv thrust sheet, Scandinavian Caledonides. Journal of Structural Geology 83, 441–455.

Grasemann, B., Stüwe, K., 2001. The development of flanking folds during simple shear and their use as kinematic indicators. Journal of Structural Geology 23, 715–724.

Grasemann, B., Stüwe, K., Vannay, J.C., 2003. Sense and non-sense of shear in flanking structures. Journal of Structural Geology 25, 19–34.

Guermani, A., Pennacchioni, G., 1998. Brittle precursors of plastic deformation in a granite: an example from the Mont Blanc Massif (Helvetic, Western Alps). Journal of Structural Geology 20, 135–148.

Hobbs, B.E., Mühlhaus, H.-B., Ord, A., 1990. Instability, softening and localization of deformation, in: Knipe, R.J., Rutter, E.H. (Eds.), Deformation Mechanisms, Rheology and Tectonics Geological Society Special Publication, 54, pp. 143–165.

Hoernes, S., Friedrichsen, H., 1974. Oxygen isotope studies on metamorphic rocks of the western Hohe Tauern area (Austria). Schweizerische Mineralogische und Petrographische Mitteilungen 54, 769–788.

Lammerer, B., 1988. Thrust-regime and transpression-regime tectonics in the Tauern Window (Eastern Alps). Geologische Rundschau 77, 143–156.

Lammerer, B., Weger, M., 1998. Footwall uplift in an orogenic wedge: the Tauern window in the Eastern Alps of Europe. Tectonophysics 285, 213–230.

Mancktelow, N.S., Stöckli, D.F., Grollimund, B., Müller, W., Fügenschuh, B., Viola, G., Seward, D., Villa, I.M., 2001. The DAV and Periadriatic fault systems in the Eastern Alps south of the Tauern window. International Journal of Earth Sciences 90, 593–622.

Morteani, G., 1974. Petrology of the Tauern window, Austrian Alps. Fortschritte der Mineralogie 52, 195–220.

Müller, G., 1967. Methods in Sedimentary Petrology. Hafner Publishing Company, New York. 283pp.

Müller, W., Prosser, G., Mancktelow, N.S., Villa, I.M., Kelley, S.P., Viola, G., Oberli, F., 2001. Geochronological constraints on the evolution of the Periadriatic Fault System (Alps). International Journal of Earth Sciences 90, 623–653.

Müntener, O., Hermann, J., 1996. The Val Malenco lower crust–upper mantle complex and its field relations (Italian Alps). Schweizerische Mineralogische und Petrographische Mitteilungen 76, 475–500.

Passchier, C.W., 2001. Flanking structures. Journal of Structural Geology 23, 951–962.

Pennacchioni, G., 1996. Progressive eclogitization under fluid-present conditions of prealpine mafic granulites in the Austroalpine Mt. Emilius Klippe (Italian Western Alps). Journal of Structural Geology 18, 549–561.

Pennacchioni, G., 2005. Control of the geometry of precursor brittle structures on the type of ductile shear zone in the Adamello tonalites, Southern Alps (Italy). Journal of Structural Geology, in press.

Platt, J.P., Vissers, R.L.M., 1980. Extensional structures in anisotropic rocks. Journal of Structural Geology 2, 397–410.

Poirier, J.P., 1980. Shear localization and shear instability in materials in the ductile field. Journal of Structural Geology 2, 135–142.

Ramsay, J.G., Allison, I., 1979. Structural analysis of shear zones in an alpinised Hercynian granite (Maggia Lappen, Pennine Zone, Central Alps). Schweizerische Mineralogische und Petrographische Mitteilungen 59, 251–279.

Ramsay, J.G., Graham, R.H., 1970. Strain variation in shear belts. Canadian Journal of Earth Sciences 7, 786–813.

Ramsay, J.G., Huber, M.I., 1983. The Techniques of Modern Structural Geology. Volume 1: Strain Analysis. Academic Press, London.

Rolland, Y., Cox, S.F., Boullier, A.M., Pennacchioni, G., Mancktelow, N., 2003. Rare Earth and trace element mobility in mid-crustal shear zones: insights from the Mont Blanc Massif (Western Alps). Earth and Planetary Science Letters 214, 203–219.

Segall, P., Pollard, D.D., 1983. Nucleation and growth of strike slip faults in granite. Journal of Geophysical Research 88, 555–568.

Segall, P., Simpson, C., 1986. Nucleation of ductile shear zones on dilatant fractures. Geology 14, 56–59.

Selverstone, J., 1984. Petrologic constraints on imbrication, metamorphism and uplift in the SW Tauern Window, Eastern Alps. Tectonics 4, 687–704.

Selverstone, J., 1988. Evidence for east–west crustal extension in the Eastern Alps: implications for the unroofing history of the Tauern Window. Tectonics 7, 87–105.

Selverstone, J., Spear, F.S., 1985. Metamorphic P–T path from pelitic schists and greenstones from the south-west Tauern Window, Eastern Alps. Journal of Metamorphic Geology 3, 439–465.

Selverstone, J., Morteani, G., Staude, J.-M., 1991. Fluid channelling during ductile shearing: transformation of granodiorite into aluminous schist in the Tauern Window, Eastern Alps. Journal of Metamorphic Geology 9, 419–431.

Simpson, C., 1983. Strain and shape-fabric variations associated with ductile shear zones. Journal of Structural Geology 5, 61–72.

Simpson, C., 1985. Deformation of granitic rocks across the brittle–ductile transition. Journal of Structural Geology 7, 503–511.

Simpson, C., 1986. Fabric development in brittle-to-ductile shear zones. PAGEOPH 124, 269–288.

Tourigny, G., Tremblay, A., 1997. Origin and incremental evolution of brittle/ductile shear zones in granitic rocks: natural examples from the southern Abitibi Belt, Canada. Journal of Structural Geology 19, 15–27.

Tremblay, A., Malo, M., 1991. Significance of brittle and plastic fabrics within the Massawippi Lake fault zone, southern Canadian Appalachians. Journal of Structural Geology 13, 1013–1023.

Urai, J.L., Means, W.D., Lister, G.S., 1986. Dynamic recrystallization of minerals, in: Hobbs, B.E., Heard, H.C. (Eds.), Mineral and Rock Deformation: Laboratory Studies. The Paterson Volume Geophysical Monograph, 36. American Geophysical Union, Washington, DC, pp. 161–199.

Van der Wal, D., Vissers, R.L.M., 1996. Structural petrology of the Ronda peridotite, SW Spain: deformation history. Journal of Petrology 37, 23–43.

Vauchez, A., 1987. The development of discrete shear-zones in a granite: stress, strain and changes in deformation mechanisms. Tectonophysics 133, 137–156.

White, S., Burrows, S.E., Carreras, J., Shaw, N.D., Humphreys, F.J., 1980. On mylonites in ductile shear zones. Journal of Structural Geology 2, 175–188.

Williams, G., Dixon, J., 1982. Reaction and geometrical softening in granitoid mylonites. Textures & Microstructures 4, 223–239.